

Jet flames from noncircular burners

S R GOLLAHALLI

School of Aerospace and Mechanical Engineering, The University of Oklahoma, Norman, OK 73019, USA
e-mail: gollahal@lincoln.ecn.ou.edu; gollahal@ou.edu

Abstract. Gas jets from noncircular exits entrain more air from surroundings than jets from circular exits of equivalent area. Because the mixing rate of fuel and air governs the combustion and pollutant emission of diffusion flames and partially premixed flames, noncircular geometries offer a passive control of the flame characteristics. In this paper, the literature on nonburning, noncircular jets is reviewed and recent studies on noncircular jet flames are discussed with focus on the work conducted in the author's laboratory.

Keywords. Gas jets; noncircular burners; jet flames; flame characteristics.

1. Introduction

Combustion and pollutant characteristics of fuel gas jets are controlled by the mixing rates of fuel and ambient air. Hence, manipulation of fluid mechanics in the vicinity of the burner mouth by varying the exit geometry appears to be an attractive method of controlling the thermochemical processes to increase combustion efficiency and reduce pollutant emission from diffusion flames. This paper presents the research on this topic with focus on the work at the University of Oklahoma.

2. Background

Noncircular exits are often considered to be passive and inexpensive methods of controlling the characteristics of isothermal jets. The geometries usually considered are elliptic, triangular, and rectangular with a small aspect ratio of 2 to 4. The nonaxisymmetric flow field tends to remove its instability by gradually becoming symmetric downstream. In the process, the smaller dimension tends to become larger and the larger dimension tends to become smaller, leading to a phenomenon called axis-switching. Before achieving symmetry, a few switchings usually occur. This characteristic of noncircular jets has been well documented (Sforza *et al* 1966; Schadow *et al* 1984; Gutmark *et al* 1985; Ho & Gutmark 1987; Hussain & Hussain 1989; Quinn 1989; Gollahalli *et al* 1992). The locations and the number of switch-overs are strongly dependent on the initial conditions, the aspect

ratio of the nozzle exit, and when excited on the flow Strouhal number. The dominance of coherent structures and azimuthal instabilities are stated as responsible for axis-switching. Koshigoe *et al* (1988) have theoretically analysed the condition for deformation of noncircular jets. The analysis of large eccentricity elliptic jets performed by Crighton (1973) has shown them to be spatially as well as temporally stable. Ho (1986) states that entrainment in two-dimensional shear layers and axisymmetric jets occurs during the vortex-merging event. In nonaxisymmetric jets, however, vortex-merging and azimuthal deformation occur simultaneously.

In comparison to the number of studies on nonreacting jets, work on the combustion of noncircular jets is severely limited. Schadow *et al* (1984) have found in a large-scale study that the combustion efficiency in elliptic jets is about 10% higher than in circular jets. Better mixing is shown to be the cause of this improvement. Gollahalli and his associates (Schadow *et al* 1984; Gollahalli & Prabhu 1990; Prabhu & Gollahalli 1990; Kamal & Gollahalli 1993; Subba & Gollahalli 1995) have investigated the structure and pollutant formation in flames of noncircular jets at various conditions. Cannon & Queiroz (1994), have studied the time-resolved temperature measurements in an elliptic turbulent diffusion flame. Recently, Papanikolaou & Wierzbka (1995, 1996) have investigated the lift-off and blow-out characteristics of diffusion flames. These studies are discussed in the following.

3. Turbulent diffusion flames

The results in this section are extracted primarily from the works of Prabhu (1989), Khanna (1990), and Kamal (1995). The experiments by Prabhu and Khanna were carried out on the same burner and experimental apparatus. Prabhu investigated the thermochemical characteristics and Khanna studied fluid mechanics of the turbulent gas diffusion flames from elliptic nozzles. Kamal recently focused his work on the coupling of burner size and exit Reynolds number on the noncircular burner effects.

3.1 *Experimental apparatus and instrumentation*

The experiments in these studies were performed in a vertical flow combustion apparatus. This facility had a combustion chamber of square cross-section (76 cm × 76 cm) and 117 cm height. The chamber had air-cooled Pyrex glass windows (20 cm × 20 cm × 92 cm) on all the side walls. While drawing gas samples and probing the temperature field, one of the glass windows was replaced with a slotted metal sheet through which the probes were introduced. The glass windows extended down to the floor level of the chamber to permit optical probing of the flames in the vicinity of the burner mouth. The burner assembly mounted to the floor of the chamber consisted of a contoured nozzle section located concentrically inside a cylindrical chamber. The fuel nozzle had four parts: a divergent inlet section, a cylindrical settling section, a convergent contoured section, and interchangeable nozzle tips. Nozzle tips of different configuration could be attached to the contraction section. Except in Kamal's work on burner size effects, a circular nozzle tip of exit diameter 9.5 mm i.d. was used. The elliptic nozzle tips (major diameter = 16.4 mm and minor diameter = 5.5 mm) had the same exit area as that of the circular nozzle. The

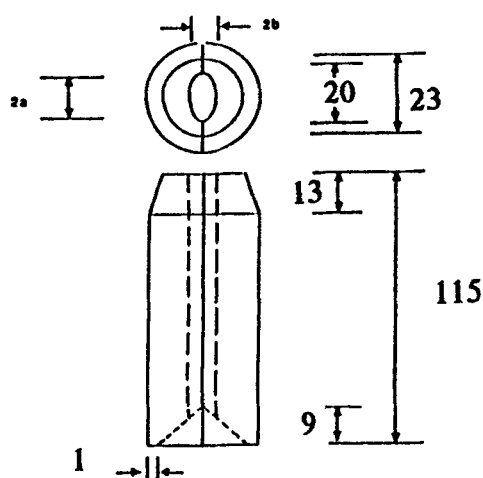


Figure 1. Details of the elliptic nozzle tips for diffusion flame studies.

ratio of the length of the elliptic cylindrical portion to the major diameter of these nozzle tips was at least 7, ensuring the ellipticity of the initial geometry of the fuel jet. Figure 1 shows the details of the elliptic nozzle tips. A mixture of propane and nitrogen was used as the jet fluid for the reason discussed later in relation to flame stability results. Combustion air was supplied from an oil-less rotary-vane compressor to the annulus surrounding the nozzle. An assembly of a honeycomb section and two sets of fine-mesh screens ensured uniform and low-turbulence air flow concentric with the fuel jet. In all experiments reported in this study the velocity of co-flow air was maintained at 0.66 m/s. The fuel jets were ignited with a pilot Bunsen flame which was withdrawn during tests.

Direct colour photography with an exposure time of 1 second was used to determine the shape and dimensions of the visible flame. A two-mirror (200 mm diameter) Z-arrangement schlieren system with a xenon stroboscopic light source of flash duration 1.5 μ s was used to visualize the flow structure in the near-nozzle region of the flames (Khanna 1990). The temperature field was probed with a thermocouple. The composition field was determined by gas sampling and analytical instruments consisting of nondispersive infrared analysers, a polarographic analyser, a chemiluminescent analyser, and a gas chromatograph. Soot concentration was determined by filtering known volumes of diluted gas samples. Radiation emitted from flames was measured with a wide view angle radiometer. The flow field in the vicinity of the flame base was probed with a laser Doppler velocimeter. Both nozzle and air-flow streams were seeded with magnesium oxide particles. A microcomputer-based data acquisition system was used to acquire and process the output data of the LDV. The details of instrumentation and error analysis are given by Prabhu (1989), Khanna (1990), and Kamal (1995). Table 1 shows the nominal experimental conditions.

3.2 Flame stability

Most of the studies on flame life-off have focused on the burner exit velocity as the primary variable. As the jet velocity affects the local flow field, flame liftoff caused by increasing burner exit velocity affects both the flow and chemical structure of the flame base region. Hence, the roles of fluid dynamics and thermochemical effects cannot be

Table 1. Nominal experimental conditions.

Type of flame	Turbulent diffusion flame	Partially-premixed flame
Fuel	Propane and nitrogen mixture	Natural gas
HHV (MJ/kg)	11–18	37.3
Energy input rate (kW)	750–1232	5.86
Fuel jet velocity (m/s)	—	49.1
Fuel jet Re_j	—	6500
Burner exit velocity (m/s)	5.60	1.275
Burner port Re_p	7810	3640
Ambient temperature (K)	297	295
Ambient pressure (mm Hg)	745	749
Ambient relative humidity	65%	65(%)

delineated. Prasad *et al* (1991) employed a method in which the lift-off phenomenon can be studied in terms of the reactant concentration in the jet fluid while keeping the burner exit velocity constant. This method is useful to isolate the effects of parameters like nozzle shape by decoupling their influences from the accompanying changes through the jet exit velocity. Hence, a mixture of N_2 and C_3H_8 was used as the jet fluid and the concentration of C_3H_8 at transitions was used as an indicator of the flame stability.

Figure 2 compares the transition characteristics of flames from circular and elliptic (aspect ratio 3 : 1) nozzles when the mole fraction of propane, x_p , in the jet stream is decreased while keeping the exit velocity approximately constant at 5.65 ± 0.30 m/s. The nominal exit velocity corresponds to a Reynolds number of 4740 in the case of the circular nozzle, and 7810 and 2620, based on the major and minor diameters in the case of the elliptic nozzle. Here L is the flame standoff distance and D_{eq} is the diameter of the circular

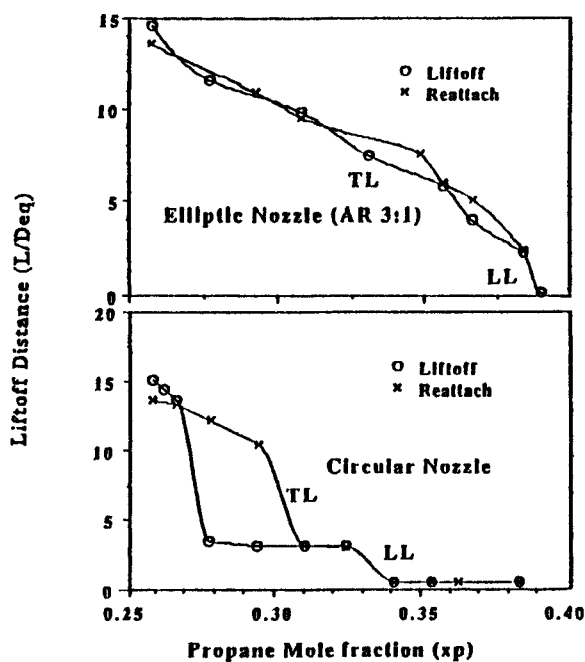


Figure 2. Lift-off and reattachment characteristics of turbulent diffusion flames from circular and elliptic nozzles.

nozzle of equal exit area. When x_p in the jet stream of the circular nozzle was above 0.34 the flame was attached to the burner. At x_p equal to 0.32, the flame base lifted off the burner and stabilized about 3 nozzle diameters above. When x_p was between 0.32 and 0.34 the flame base position was not well-defined and the flame was seen to be detached from only a part of the nozzle rim. The flame edges appear smooth and the flow near the flame base appears laminar. This transition is denoted as “Laminar Liftoff” and is shown as LL on the figure. When propane mole fraction is further decreased to 0.28, the liftoff height suddenly increases to about 10 diameters while the flame base widens to about 4 nozzle diameters. Flow near the flame base is turbulent in this configuration. This transition is denoted as “Turbulent Liftoff” and is indicated as TL on the figures. When x_p is decreased further L increases slowly before flame blows out at $x_p = 0.24$. With the elliptic nozzle, the first transition LL occurs at $x_p = 0.38$, the second transition TL occurs at $x_p = 0.33$, and flame blows out at $x_p = 0.24$. This shows that elliptic nozzle flames require more reactive component in the jet fluid to avoid transitions of burner-attached flame to liftoff and blowout conditions than circular nozzle flames. Also, the flame-standoff distance does not remain constant between the first and second transitions in the elliptic nozzle flames, in contrast to the circular nozzle flames.

When propane mole fraction in the jet fluid is increased while the flame from the circular nozzle is in the lifted condition, the L/D_{eq} versus x_p curve does not retrace its path and exhibits hysteresis similar to the hysteresis noticed in earlier studies (Scholfield & Garside 1949; Gollahalli *et al* 1987). In those studies, the differences in the turbulence characteristics of the flame-standoff region upstream of the flame base between the attached and lifted flames were thought to be responsible for the hysteresis. The hysteresis behaviour, however, is not significant in the flame from the elliptic nozzle. The earlier initiation of instabilities and consequently higher turbulence level in the elliptic nozzle jets seem to be responsible for the negligible hysteresis in the liftoff-reattachment characteristics of the elliptic nozzle flame.

3.3 Fuel concentration profiles

The axial concentration profiles of propane in the attached flames from circular and elliptic nozzles are shown in figure 3. We notice that fuel concentration decreases more slowly along the axis and the fuel persists longer in the circular nozzle flame than in the elliptic

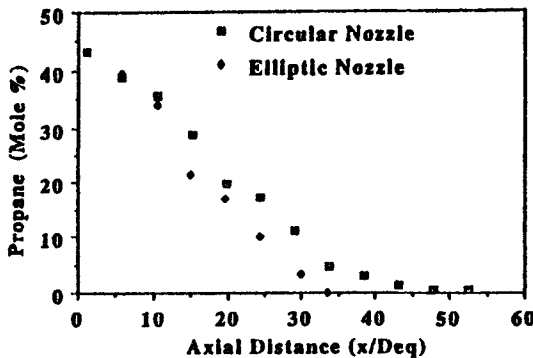


Figure 3. Effect of nozzle shape on the axial concentration profiles of fuel in turbulent diffusion flames from circular and elliptic nozzles.

nozzle flame. For instance, the value of x_p decreases to 0.005 at $x/D = 48$ in the circular nozzle flame, whereas the same value is reached at $x/D_{eq} = 34$ in the elliptic nozzle flame. The rapid depletion of propane is caused by the greater dilution due to the higher entrainment in the elliptic nozzle flame.

3.4 *Temperature profiles*

Figure 4 shows the radial temperature profiles at three axial levels in the circular and elliptical nozzle flames attached to the burner. These locations are in the near-nozzle, midflame, and far-nozzle regions of the flames. In both flames the near-nozzle profile has a sharp off-axis peak. A comparison of these profiles reveals that the circular nozzle flame has a slightly higher peak temperature compared to the elliptic nozzle flame in the near-nozzle region. However, in the midflame and far-nozzle regions, the elliptic nozzle flame has higher peak values. As homogeneous gas phase reactions are dominant in the near-nozzle region, the more rapid development of a shear layer and the higher degree of mixing with air in the elliptic nozzle flame could lead to a lower peak temperature. On the other hand, in the midflame and far-nozzle regions, the kinetics-controlled heterogeneous soot oxidation reactions are the primary mechanisms of heat release (Gollahalli 1977). These kinetics-controlled processes are enhanced in the elliptic nozzle flame by the larger oxygen availability, thereby leading to higher rates of burning of soot. The higher heat release rates and the lower heat loss rates due to lower concentrations of soot result in higher temperatures in the midflame and far-nozzle regions of the elliptic nozzle flame, compared to the temperatures in the corresponding regions of the circular nozzle flame. It appears that the dilution effect of increased entrainment of air into the flame is overshadowed by the enhancement of soot combustion which results in higher temperature in the midflame and far-nozzle regions of the elliptical nozzle flames. The differences in the jet growth rate determined from velocity measurements in circular and elliptic nozzle flames presented later are in conformity with the temperature profiles.

3.5 *Nitric oxide and particulate concentration profiles*

Figure 5 shows the radial concentration profiles of nitric oxide at three axial levels in the attached flames from the circular and elliptic nozzles at the same conditions at which the temperature field was probed. Except in the far-nozzle regions, the differences in the peak concentration of nitric oxide in the circular and elliptic nozzle flames follow the trends of temperature profiles discussed above, as expected of thermal nitric oxide produced through Zeldovich reactions. In the near-nozzle region, the peak concentration of nitric oxide is higher in the circular nozzle flame, because of the thinner interfacial reaction zone that results in a higher peak temperature than in the near-nozzle region of the elliptic nozzle flame. In the midflame region, the elliptic nozzle flame has a higher nitric oxide concentration than the circular nozzle flame, which also follows the trend of temperature. In the far-nozzle region, the average of the NO concentrations on the major and minor axes of the elliptic nozzle is slightly less than the NO concentration level in the circular nozzle flame.

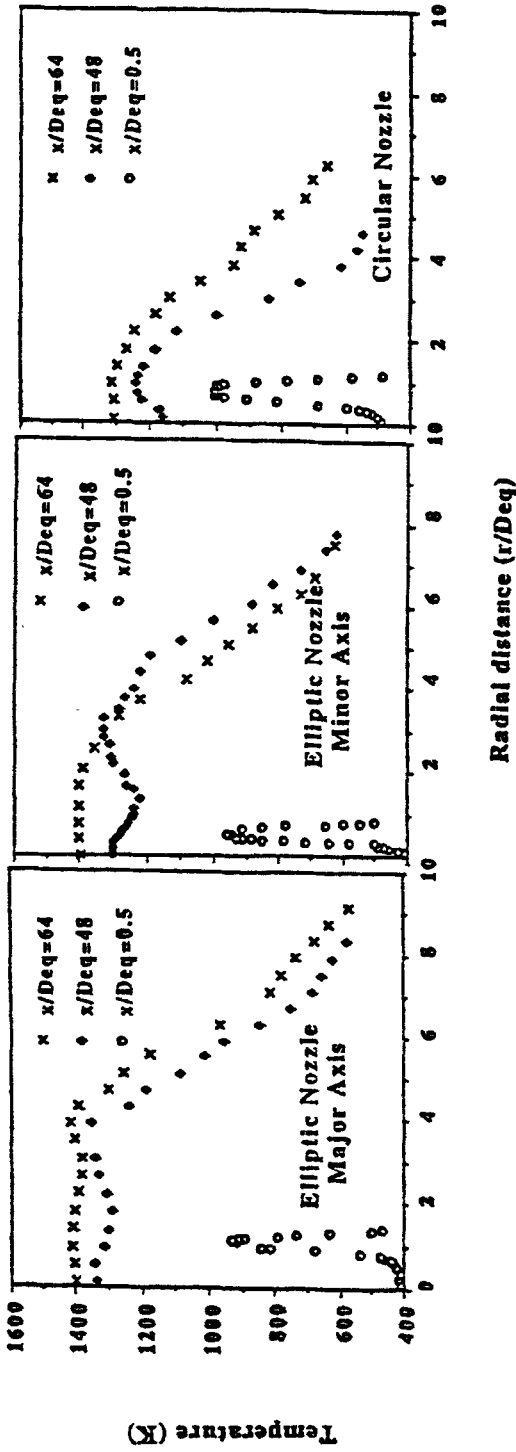


Figure 4. Radial temperature profiles in turbulent diffusion flames from circular and elliptic nozzles.

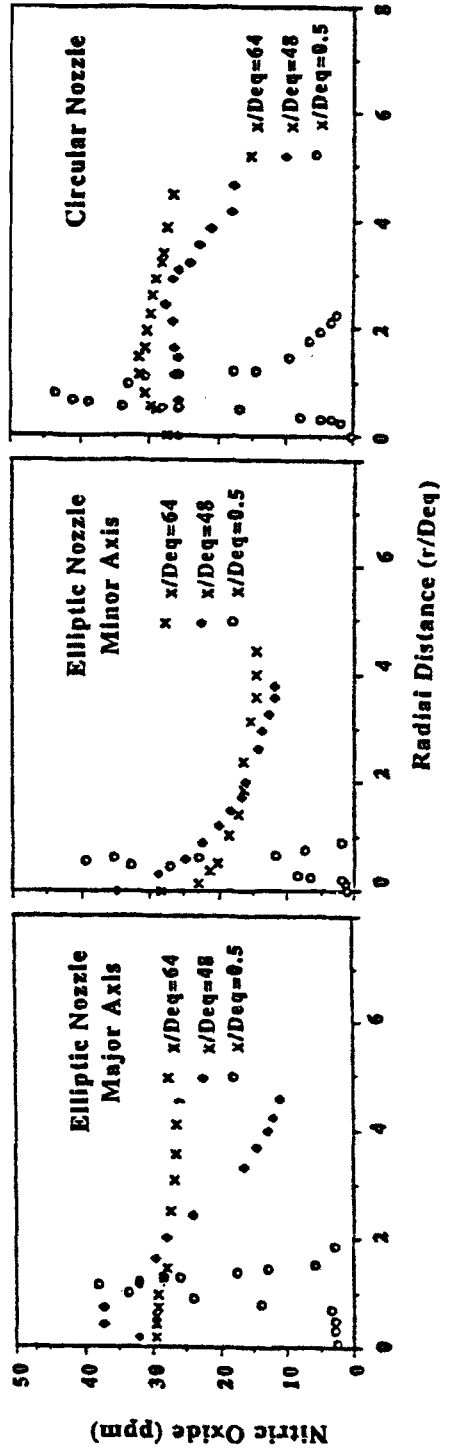


Figure 5. Radial nitric oxide concentration profiles in turbulent diffusion flames from circular and elliptic nozzles.

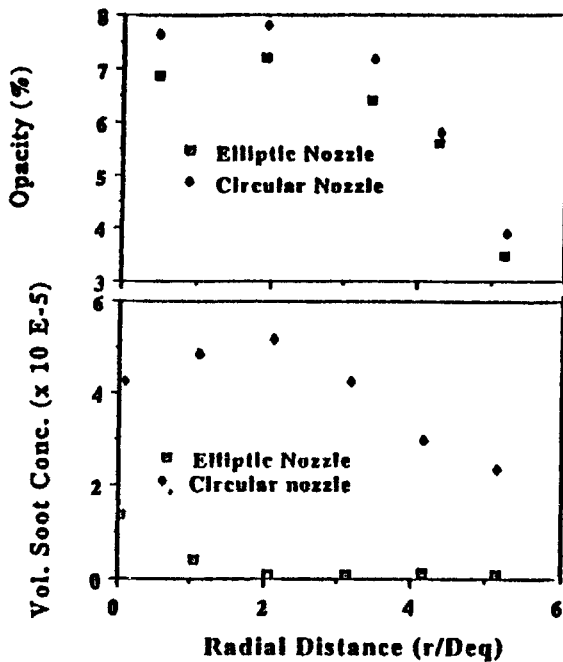


Figure 6. Effects of nozzle shape on soot concentration and opacity in turbulent diffusion flames from circular and elliptic nozzles.

The radial variations of particulate concentration and opacity of the combustion product samples drawn from the far-nozzle regions of the circular and elliptic nozzle flames are shown in figure 6. Clearly, soot concentration in the elliptic flame is smaller than in the circular flame. The difference in the opacities of samples from the two flames is not as large as the difference in the mass concentration of soot, probably because of the variance in the size distribution of the particulates. The lower soot concentrations in the elliptic nozzle flame are in conformity with the effects expected from the higher entrainment of air. The higher entrainment of air (Gutmark *et al* 1985) promotes soot oxidation rates in the far-nozzle region. Consequently, the particulate concentration in the elliptic nozzle flame is lower.

3.6 Nitrogen oxides emission index

Figure 7 shows the comparison of the emission index (EI) of NO_x of the circular and elliptic nozzle flames. The values of emission index (ng/J) of elliptic nozzles are normalized with the emission index of circular nozzle. The letter E corresponds to the elliptic nozzle and the number following the letter E refers to its aspect ratio. It is clear from the figure that in turbulent diffusion flames the EINO_x is not significantly different for elliptic and circular nozzles. This can be traced to the opposing variations of the peak NO_x concentrations in different regions of the flame. The smaller value of EINO_x reflects the trends of the NO concentrations in the far-nozzle region. The degree of reduction, however, varies substantially and is highest for the nozzle of aspect ratio 2.

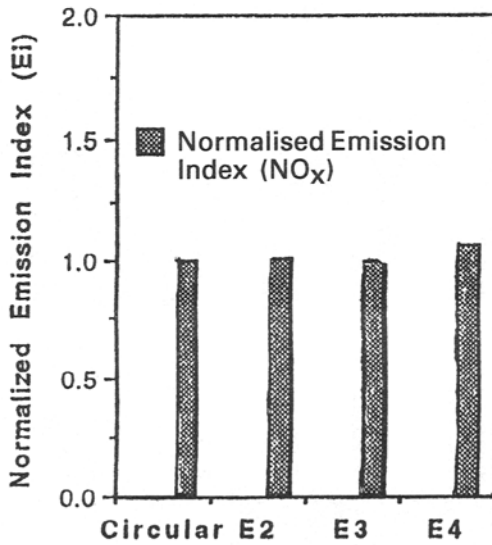


Figure 7. Comparison of nitric oxide emission index in turbulent diffusion flames from circular and elliptic nozzles.

4. Laminar partially premixed flames

The studies presented here on this topic are taken from the works of Kolluri (1992), Rao (1994), and Subba (1995). The natural gas furnaces of residential and commercial heating systems employ partially premixed laminar flame burners. These burners are operated with low supply pressures, typically of the order of a few centimeters of water column, and combustion occurs generally at atmospheric pressure. Hence, the designer's choice of varying the operating parameters to control fuel-air mixing rates and pollutant emission characteristics of these burners is severely limited. Motivated by the argument that air entrainment into isothermal gas jets can be significantly altered by the passive approach of using the noncircular geometries for the nozzle exit, a research program in the author's laboratory has been focused on changing the shapes of various crucial components of an inshot gas burner of a residential natural gas furnace to noncircular geometry. The exhaust emission indices of NO, NO_x, and CO, in-flame profiles of temperature and species concentrations, air entrainment rate, and flow patterns have been studied for noncircular geometries (elliptic, triangular, and rectangular) of fuel nozzles, venturis, and burner exit ports. The discussion here is limited to only *elliptic* geometries of the *burner exit port*.

4.1 Burner apparatus

Figure 8 shows the sketch of an inshot burner rated at 5.46 kW used in a natural gas-fired residential furnace. Experiments were conducted in the combustion chamber and the instrumentation facilities described in § 3.1. The natural gas was supplied from the lab supply line and heating values were monitored on a daily basis. The fuel flow rate to the burner was adjusted in order to keep the energy input rate to the burner constant. The flow velocity and the area of the elliptic burners were maintained the same as those of the circular burner, and hence the observed changes in flame characteristics could be

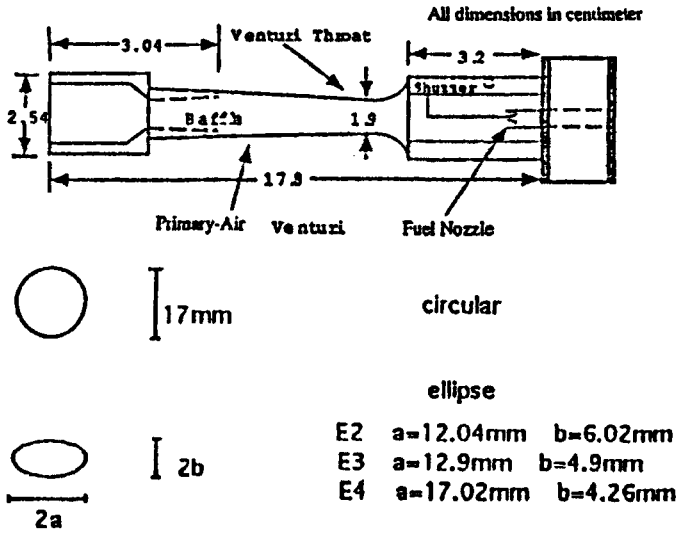


Figure 8. Sketch of the inshot burner with standard and modified tips.

attributed to only the shape of the burner exit port. Table 1 also contains the experimental conditions in this series of studies.

4.2 Results

Figure 9 shows the effects of elliptic geometry of the burner tips on the ambient air-entrainment into the nonburning jets. Entrainment rate was determined by measuring the concentration of oxygen at $15 D_{eq}$ corresponding to the visible flame length. It is clear that the elliptic burner tips increase air-entrainment by as much as 30%. More interestingly, the entrainment change is not monotonic with the aspect ratio of the burner tip. The shadowgraph pictures of the flames (Subba 1995) with the standard circular and noncircular burner tips show that the flow emerging from the burner port has azimuthal instabilities

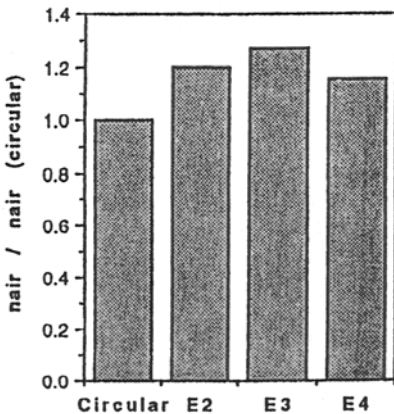


Figure 9. Air-entrainment into the partially premixed flames of circular and elliptic tip burners.

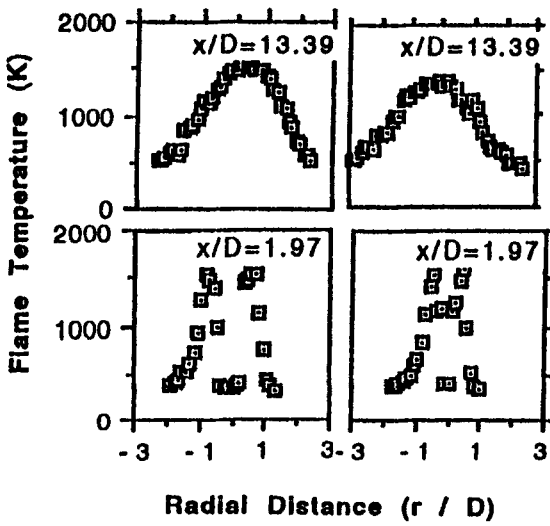


Figure 10. Comparison of temperature profiles in the partially premixed flames of circular and elliptic tip burners.

indicated by the axial streaks in both flames. However, the elliptic burner flame shows more numerous streaks confirming that the azimuthal instabilities are enhanced by the elliptic geometry of the burner.

Figure 10 shows the temperature profiles in the near- and far-nozzle regions of the flames of the circular and the elliptic burners. It is clear that the trends of these profiles are strikingly similar indicating that there is no dramatic shift in the dominant physico-chemical processes due to the shape of the burner tips. The peak values of far-nozzle temperature in the elliptic burner flames, although not conspicuous in the figure because of the compressed scale, are lower than in the circular burner flames. This decrease can be attributed to the higher air-entrainment and lower soot production in the elliptic burner flames. In the near-nozzle region, the temperatures are not significantly different in the

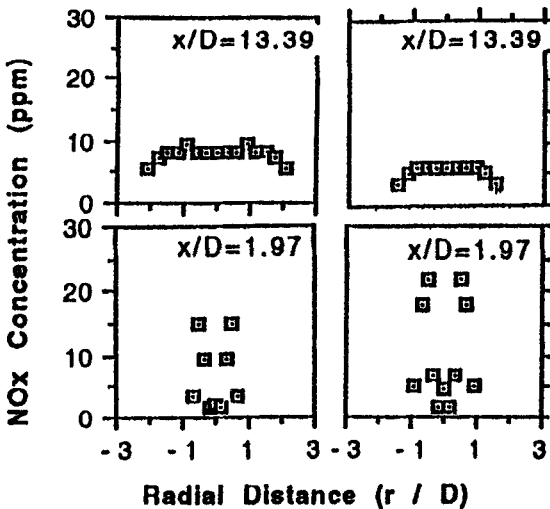


Figure 11. Comparison of nitrogen oxide concentration profiles in the partially premixed flames of circular and elliptic tip burners.

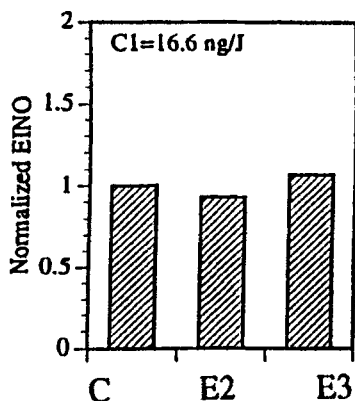


Figure 12. Nitrogen oxides emission index in the partially premixed flames of circular and elliptic tip burners.

two flames, presumably due to the fact that the increase in the oxidation rates of the fuel pyrolysis fragment species compensates for the increased dilution caused by the higher air-entrainment in that region.

Figure 11 shows the NO_x concentration profiles in the circular and the elliptic nozzle (aspect ratio 4) flames. Similar to the temperature profiles, the NO_x concentration profiles also show double hump structure in the near-nozzle and midflame regions and either flat or single axial peak structure in the far-nozzle region. It is clear that interfacial combustion at the flame edges continues to be dominant until the midflame region. In conformity with the temperature profiles and entrainment results, the values of the peak NO_x concentration in the far-nozzle region are generally lower in the elliptic burner flame.

Figure 12 shows the effect of burner shape on emission indices of NO_x . It is clear that the elliptic shape E2 has a favorable effect on the pollutant emission indices of the burner, although the effect is less than about 15%.

5. Concluding remarks

Flow visualization studies of the structure of gas jets and flames have shown that the large scale coherent structures initiated by Kelvin–Helmholtz instabilities are responsible for the entrainment of surrounding fluid (Ho & Gutmark 1987). Also, it has been shown that noncircular geometries of the nozzles introduce many azimuthal instabilities which interact with these organized structures, and consequently, produce differential radial growth rates of jet and the consequent axis switching. Thus, air-entrainment rate and combustion characteristics of flames are affected by the noncircular shape of the burner, which has been demonstrated in the case of turbulent propane *diffusion* flames. Although the *partially premixed* flames were laminar, the results show that somewhat similar features exist. Since the burner exit conditions were such that the flames were not fully turbulent, the effects on entrainment and temperature field in this case seem to be smaller than in the turbulent case. The higher air-entrainment into the near-nozzle region increases the oxidation of the pyrolysis species of the fuel and reduces soot formation rate. Further, the additional dilution also reduces peak temperatures and consequently leads to lower concentrations of nitrogen oxides.

The funding for the studies from which the material for this paper is extracted was provided by the Gas Research Institute, Chicago, Illinois and the Oklahoma Center for Advancing Science and Technology, Oklahoma City, Oklahoma in USA.

References

- Cannon S M, Queiroz M 1994 Time resolved temperature measurements in an elliptic cross-section, turbulent diffusion jet flame. *ASME Winter Annual Meeting*, Chicago, IL, ASME vol. HTD 296, pp 37–45
- Crighton D G 1973 Instability of an elliptic jet. *J. Fluid Mech.* 59: 665–672
- Gollahalli S R 1977 Effects of diluents on the flame structure and radiation of propane jet flames in a concentric stream. *Combustion Sci. Technol.* 9: 147–160
- Gollahalli S R, Prabhu N 1990 Differences in the structure of lifted gas jet flames with laminar base over circular and elliptic nozzles. *Emerging Energy Technology Symposium*, New Orleans, LA, ASME Paper No. 90-Pet-14
- Gollahalli S R, Savas O, Huang R, Rodriguez Azara J L 1987 Flow structure of a lifted gas jet flame in the hysteresis region. *Twenty-first symposium on Combustion* (Philadelphia: The Combustion Institute) pp 1463–1471
- Gollahalli S R, Khanna T, Prabhu N 1992 Diffusion flames of gas jets issued from circular and elliptic nozzles. *Combustion Sci. Technol.* 86: 267–288
- Gutmark E, Schadow K C, Wilson K J 1985 The mean and turbulent structure of noncircular jets. *AIAA Conference*, Colorado Springs, CO, AIAA Paper No. 85-0543
- Ho C M 1986 Mixing processes in free shear layers. *24th Aerospace Sciences Meeting*, Reno, NV, AIAA Paper No 86-0234
- Ho C, Gutmark E 1987 Vortex interaction and mass entrainment in a small aspect ratio elliptic jet. *J. Fluid Mech.* 179: 383–405
- Hussain F, Hussain H S 1989 Elliptic jets: part 1; Characteristics of unexcited and excited jets. *J. Fluid Mech.* 208: 257–320
- Kamal A 1995 *Turbulent diffusion gas jet flames from circular and elliptic nozzles*, Ph D dissertation, University of Oklahoma, Norman, OK
- Kamal A, Gollahalli S R 1993 Effects of noncircular fuel nozzles on the pollutant emission characteristics of natural gas burners for residential furnaces. *International Joint Power Conference*, ASME vol. FACT 17, pp 41–50
- Khanna T 1990 *Flow structure of jets and flames over elliptic nozzles*, M S thesis, University of Oklahoma, Norman, OK
- Kolluri P 1992 *The study of the interaction of noncircular venturi inlets with circular fuel jet in the inshot burners of natural gas furnaces*. M S thesis, University of Oklahoma, Norman, OK
- Koshigoe S, Gutmark E, Schadow K C, Tubis A 1988 Instability analysis on noncircular free jets. *26th Aerospace Sciences Meeting*, Reno, NV, AIAA Paper No. 88-0037
- Papanikolaou N, Wierzbka I 1995 Effect of burner geometry on the blowout limits of jet diffusion flames in a co-flowing oxidizing stream. *Emerging Energy Technology Symposium*, Houston, TX, ASME vol. PD-66, pp 29–36
- Papanikolaou N, Wierzbka I 1996 Effect of burner geometry and fuel composition on the stability of a jet diffusion flame. *Emerging Energy Technology Symposium*, Houston, TX, (in press)
- Prabhu N 1989 *Gas jet flames over elliptic nozzles*, M S thesis, University of Oklahoma, Norman, OK
- Prabhu N, Gollahalli S R 1990 Effect of aspect ratio on combustion characteristics of elliptic nozzle flames. *Emerging Energy Technology Symposium*, ASME vol. PD-36, pp 51–56

- Prasad A, Gundavelli S, Gollahalli S R 1991 Characteristics of diluent-caused lifted gas jet flames. *J. Propulsion Power* 7: 659–667
- Quinn W R 1989 The turbulent free jet issuing from a sharp edged elliptic slot. *27th Aerospace Sciences Meeting*, Reno, NV, AIAA Paper No. 89-0664
- Rao A V 1994 *Effects of venturi inlet geometry on combustion characteristics of inshot burners used in residential gas furnace systems*. MS thesis, University of Oklahoma, Norman, OK
- Schadow K C, Wilson K J, Lee M J 1984 Enhancement of mixing inducted rockets with elliptic gas generator nozzles. *20th Joint Propulsion Conference*, Cincinnati, OH, AIAA Paper 84-1260
- Scholfield D A, Garside J E 1949 Structure and stability of diffusion flames. *Third International Symposium on Combustion*, pp 102–109
- Sforza P M, Steiger M H, Trentacoste N 1966 Studies on three-dimensional viscous jets. *AIAA J.* 4: 800–806
- Subba S 1995 *Effects of burner exit geometry on combustion characteristics of inshot burners used in residential gas furnace systems*. MS thesis, University of Oklahoma, Norman, OK
- Subba S, Gollahalli S R 1995 Flame structure and pollutant emission characteristics of noncircular partially premixed laminar gas jets. *Third Asian Pacific International Symposium on Combustion and Energy Utilization*, Hong Kong